Journal of Natural Sciences and Mathematics
Qassim University, Vol. 8, No. 2, pp 133-152 (July 2015/Ramadan 1436H.)

Effect of Ion Implantation on some Physical Properties of Nitinol (Ni-Ti) Shape-Memory Alloy: A Review

Z. H. Dughaish

Department of Physics, College of Science,
Qassim University, PO Box 6644, Buraidah 51452, Qassim, Saudi Arabia
E-mail: msary@qu.edu.sa., zhdalmas45@gmail.com.

Abstract. Shape-memory alloys (SMAs) are unique class of metal alloys that after a large deformation can, on heating, recover their original shape. Its non-linear behavior and thermal dependence attracted many researchers, engineers and designers to choose the right material for proper applications in many fields of industry. The most commonly used material is nitinol (NiTi). Nitinol is highly biocompatible and has suitable properties for use in orthopaedic implants. Due to Nitinol's unique properties it has seen a large demand for use in less invasive medical devices. Nitinol tubing is commonly used in catheters, stents, superelastic needles and in devices for reconnecting the intestine after removing the pathology. Nitinol has been increasingly utilized in a variety of medical devices, actuators and robotic industries, nuclear reactors, in radiation environment, nuclear industry and other applications. During service in nuclear reactors, nitinol is exposed to many types of radiations which may affect its properties and structure. A comprehensive collection of previous reports on the effects of ion implantation of different energetic massive species: He^{+}, B^{+}, C^{+}, N^{+}, Ar^{+}, Xe^{+}, Ti^{+2}, Ni^{+2}, Cu^{+2} and Au^{+3} on nitinol properties are given. I hope this will be a useful and helpful guide to researchers and engineers working in this field.

Keywords. Shape memory alloys. Nitinol. NiTi. Radiation effects. Metals and alloys. Phase transformation. Martensite transformation. Ion implantation

PACS. 73.61.At; 74.25.Fy; 81.40.Wx

1. Introduction

Shape memory alloys (SMAs) are metals that "remember" their original shapes. SMAs are useful in manufacturing endovascular stents, biomedical and surgical devices [1-8], robotic actuators and fastening mechanisms [9-21]. The shape-memory phenomenon, allows devices made of nitinol (NiTi) to assume one shape when cold and another when heated.

Nitinol exhibits the highest efficiency among other shape memory alloys such as: gold-cadmium, indium-thallium, and copper-zinc. At temperatures below the transition temperature $T_{C,}$ it has excellent corrosion resistance, nonmagnetic nature, low density and high fatigue strength. TiNi shape memory alloys (SMAs) of near equiatomic composition are of technological importance. Nitinol is highly biocompatible and has properties suitable for use in orthopaedic implants. Due to Nitinol's unique properties, it has seen a large demand for use in less invasive medical devices. Nitinol tubing is commonly used in catheters, stents, superelastic needles and in devices for reconnecting the intestine after removing the pathology. There is an interest in Ni-rich NiTi alloys because the phase transformation temperatures can be controlled through heat treatment [22, 23].

Many researchers had studied the martensitic and austenitic transformations in nitinol [24-31] using different techniques: differential scanning calorimetry (DSC), positron annihilation technology (PAT) and transmission electron microscopy (TEM), X-ray diffraction (XRD) and neutron diffraction (ND). They found that increasing the stress would also increase the martensitic to austenic (MA) transformation temperatures A_S and A_F (A_S start and A_F finish) [29]. A_S and A_F decrease with increasing annealing temperature due to the reduction in the dislocation density and internal stress and agrees well with the result of Miller et al. [25].

He et al. [30] studied the influence of both stress and material state on the phase transformation, and put a phase diagram to describe the SMA response and for subsequent modeling and predictions.

The B19' (cubic) of NiTi is unstable and cannot store shape memory at the atomic level [31], however, the B19' structure can be stabilized by a wide range of applied or residual stresses. In TiNi alloy thin films [32] the activation energy of TiNi alloy increases linearly with pressure and Ti-concentration in a different manner than the bulk TiNi alloy.

More details of all aspects of SMAs from fundamentals to applications are available in some books [33-36]. Application of SMA in biomedical industry and related fields is found in Refs. [37, 38].

Irradiation of matter with energetic particles can induce disordering and amorphization in certain intermetallic compounds [39-43]. Brimhall [44] and Maziaz et al. [45] showed that the crystallization temperature of amorphous alloys is significantly lowered by heavy ion and electron irradiation. Kinoshita [46] studied the electron irradiation-induced transformation in alloys and ceramics. Precipitate-

free zones (PFZs) were observed in the thinner part of the foil or in the near-surface regions when the irradiation temperature was in the range 600-700 ^{o}C [47]. At higher temperature of 800 ^{o}C, precipitation took place preferentially at the foil surfaces. Electron irradiation affects the sink efficiency of the foil surfaces.

Effects of electron irradiation on Nitinol are available in Refs. [44-50], proton irradiation effects are found in Refs. [51-61], and neutron irradiation effects are found in Refs. [62-68].

Nanocrystalline (NC) materials can exhibit enhanced irradiation resistance. Fully dense NC TiNi alloys can be produced by severe plastic deformation (SPD) and subsequent annealing [69]. NC TiNi with a long-range ordered B2-phase (cubic) is an attractive material to study irradiation with energetic particles and its effects on the stability of the ordered super lattice. Ordered alloys allow the use of averaging techniques, such as XRD to determine irradiation effects by following disordering or amorphization instead of the time-consuming microscopic methods needed to study individual defects, such as dislocation loops, in regular metals and alloys.

When NC TiNi and NC Cu-0.5 % Al_2O_3 alloys, produced by SPD- method, were irradiated by high proton doses no defects were observed [70]. The damage, expressed in density of point defect clusters observed by TEM, decreased by a factor of 3-4 when the grain size was reduced from 100 nm to 40 nm, and no defects were found when the grain size was less than 20 nm [71]; which confirms that NC TiNi exhibits radiation resistance.

2. Implantation Effects of Inert Gas Ions (He^+, Ar^+ and Xe^+) on NiTi Alloys Properties

Irradiation of NiTi alloy thin films (2-4 μm) by very low doses of He^+ (atomic weight 4.0026) even below 0.01 dpa, affected the premartensitic transformation; and the characteristic temperatures were significantly lowered [71]. The two-way shape memory effect present in the film before irradiation was still observed even after a damage of 0.01 dpa [72].

Fully dense NC $Ti_{49.4}Ni_{50.6}$ (23-31nm) and coarse grained (CG) $Ti_{49.4}Ni_{50.6}$ alloys were subjected to the same damage dose of 1.5 MeV Ar^+ (atomic weight 39.948) at room temperature with ion flux of 6.4 x 10^{12} ions cm^{-2} s^{-1} [73]. NC TiNi retained the long-range order while the coarse-grained counterpart was amorphous. The lattice of NC TiNi still exhibits a substantial degree of long range order, while the CG structure shows considerable amorphization at a quarter of the damage dose. Internal pores are efficient sinks for the ion-induced defects. It is concluded that bulk crystalline compacts with residual porosity exhibit considerable tolerance to irradiation. Fully dense NC TiNi exhibit enhanced ion irradiation resistance which provides an evidence for the important role of the internal interfaces to reduce or even prevent the accommodation of radiation damage [73]. The total ion damage necessary to initiate the long-range disordering of bulk NC TiNi alloy is at least one

order of magnitude higher as compared to CG TiNi, which is already partially amorphized at a dose of 0.4 dpa.

Irradiation of TiNiCu SMA by 400 keV Xe^{+} (atomic weight 131.293) caused amorphization at ~ 0.4 dpa and the recrystallization started when annealed at 277 ^{o}C and basically finished at 750 ^{o}C [74].

3. Implantation Effects of B^{+}, C^{+}, N^{+}, Ti^{+2}, Ni^{+2} and Au^{+3} Ions on NiTi Alloys Properties

Heavy ion irradiation alters the crystallization mode by causing direct transformation to the final equilibrium phase as opposed to intermediate metastable phase formation during thermal annealing or electron irradiation. The equilibrium phase is believed to nucleate directly in the displacement cascades, which only form during heavy ion bombardment. Binary and multi-element amorphous alloys showed this type of response to irradiation. Radiation enhanced diffusion processes in the amorphous state can explain the increased crystallization kinetics during irradiation.

Boron (B^{+}) and nitrogen (N^{+}) ions (atomic weights 10.810, 14.007, respectively) implantation were used to improve the mechanical properties of NiTi alloys and study their effects on the chemical and physical properties [75]. Low nitrogen and boron implantation doses have no important effects on hardness (H) and elastic modulus (E), Table 1 and Fig. 1, where R is a dimensionless parameter, can be directly deduced from the load – displacement curve, defined as:

$$R\ (\%) = 100\ (h_T - h_R / h_T) \qquad (1)$$

Where h_T and h_R are the total indentation depth and the depth of the residual imprint, respectively.

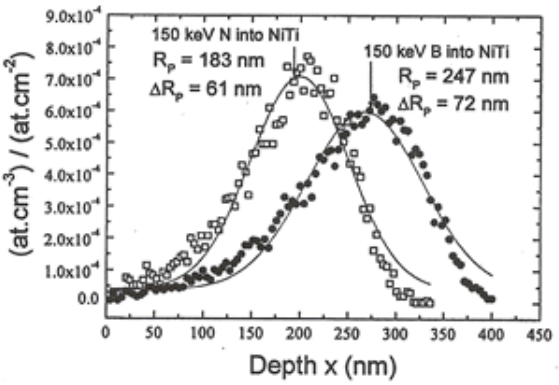

Figure (1). Concentration distribution of boron and nitrogen atoms in NiTi alloy simulated with TRIM after implantation at E = 150 keV, Reference [76].

Table (1). Implantation parameters of the investigated samples and the corresponding values of mechanical properties deduced from load-displacement curves obtained with nano-indentation, C_{max} is the maximal concentration of the implanted atoms, R is the elastic recovery, Reference [76].

Samples	Dose (at. cm^{-2})	C_{max} (at.%)	Elastic recovery R (%)	Hardness H (GPa)	Elastic modulus E (GPa)
B1	1.0×10^{16}	0.64	31.3	7.00	103
B2	5.0×10^{16}	3.10	35.6	7.25	95
B3	1.0×10^{17}	6.01	33.1	7.70	110
N1	1.0×10^{16}	0.94	33.3	6.30	91
N2	5.0×10^{16}	4.53	33.7	7.55	104
N3	1.0×10^{17}	8.66	34.9	7.30	102

The hardness profiles exhibit characteristics evolutions with applied load P_{max}, already observed after B^+, N^+, and C^+ (atomic weight 12.011) ion implantation into titanium alloys, Fig. 2 [75,76]. The hardness and elastic modulus values had been determined from characteristic load – displacement curves Fig. 2a. Figure 2b represents the evolution of hardness (H) and elastic modulus (E) as a function of penetration depth for the unimplanted NiTi alloy. Pelletier et al. [76] noted different evolutions of chemical and structural transformations as a function of ion species and implanted dose.

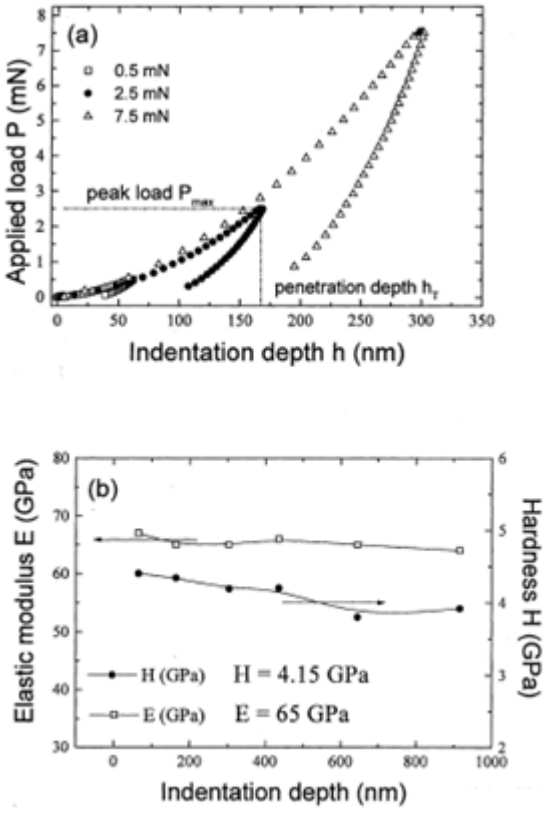

Figure (2). Mechanical properties of the used superelastic NiTi alloy, with (a) the characteristic load-displacement curves and (b) evolutions of hardness and elastic modulus profiles, measured with nanoindentation tests on unimplanted NiTi sample, Reference [76].

Grazing incidence X-ray diffraction (GIXRD) measurements, Fig. 3 [76], showed a significant increase of the mechanical properties due to the formation of a partial amorphous layer around the ion projected. The formation of this amorphous layer seems to be independent of the implanted species and dose. In NiTi alloy partial restoration phenomenon and recrystallization may happen. It is expect [76] that wear resistance of NiTi surface, and the endodontic instruments may be also enhanced by boron or nitrogen implantation. Figure 3a shows that the *B*2 austenite phase, for N^+ implantation, is always present at each dose and also shows an important shoulder at small 2θ angles on the (110) main lines of austenite for the specimen implanted at 5×10^{16} N^+ cm^{-2}, where no *B*19' martensitic phase was detected.

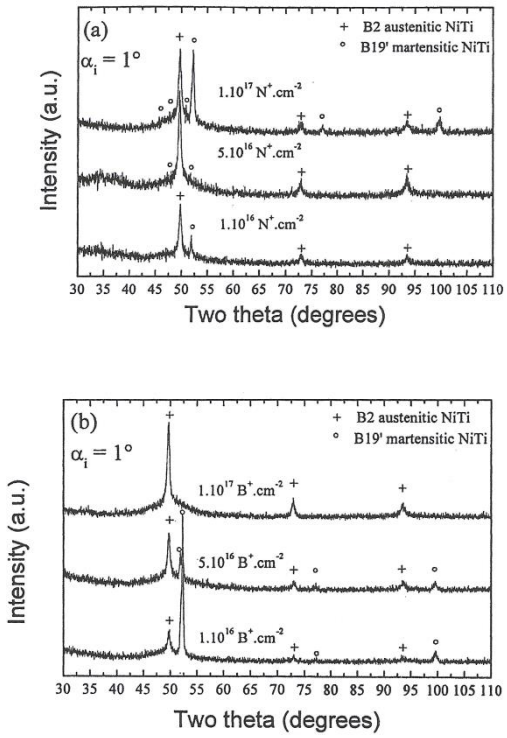

Figure (3). GIXRD patterns at fixed angle α_i = 1º showing the influence of nitrogen (a) and boron (b) implanted doses, Reference [76].

The peak broadening was attributed to partial amorphization of initial *B*2 austenitic phase, rather than implanted N^+. Figure 3b, for B^+ implantation, shows the main peaks corresponding to the *B*2 austenite are still present and the relative intensities I_M/I_A, with I_M and I_A the integrated intensities of the martensitic and austenitic phases, respectively, decreases with the implanted dose showing a strong decrease of the *B*19' marensitic concentration in the implanted layer with increasing boron dose. B^+ implantation into nitinol alloy improved the surface hardness of the alloy [76]; boron-implanted and unimplanted (pure) nitinol alloys have surface hardness of 7.6 ± 0.2 and 3.2 ± 0.2 GPa, respectively, at the nano indentation depth of 0.05 μm. The hardness of the ion-beam-modificated nitinol alloy exceeds the surface hardness of stainless steel, Table 2 [76].

Table (2). Comparison between physical and mechanical properties of NiTi alloy and stainless steel, Reference [76].

Recovered elongation (a.u.)	Ultimate Tensile stress (MPa)	Hardness H (GPa)	Elastic Modulus *E* (GPa)	Density (g cm^{-3})	Material
8%	1240	4.15±0.5	65 ± 3	6.45	NiTi alloy
0.8%	760	3.50±0.5	210 ±5	8.03	316L stainless steel

TEM and XRD studies of plastically deformed martensitic TiNi thin films irradiated with 5 MeV Ni-ion (Ni^{2+}) (atomic weight = 58.693) and various fluences and temperatures showed a continuous amorphous matrix. Irradiations to similar doses of Ni^{+2} at 150, 200, and 250 ^{o}C showed that the amorphization kinetics slow down appreciably as the temperature is increased in this range. No amorphization was detected at irradiation temperatures T ≥ 350 ^{o}C, even after doses of 4 dpa [45,77-78]. Ion implantation in $Ti_{49.5}Ni_{50.5}$ SMA with modified surfaces by the high-dose ion implantation (HDII) technique was done in two stages: with Cu-ions (Cu^{+2}) (atomic weight = 63.546) then with Ti-ions (Ni^{+2}) of equal energy (60 keV) [79]. The incident doses were: 0.7 x 10^{17}, 1.4 x 10^{17} and 2.1 x 10^{17} ion cm^{-2} for Cu^{+2} and 1 x 10^{17} ion cm^{-2} for Ti^{+2}. The temperature of the implanted samples did not exceed 100 - 151 ^{o}C. The depth of an oxide layer did not exceed 10 nm in the polished samples, while in the irradiated samples it was more than 50 nm.

The depth of an oxide layer did not exceed 10 nm in the polished samples, while in the irradiated samples it was more than 50 nm. In the irradiated TiNi samples, nickel was absent in the surface layer down to a depth of ~ 30-40 nm, Fig. 4 [79], and its content increased slowly to ~ 50 at % to the depth of 70-100 nm. It is concluded that a special surface layer is formed under the irradiated side with chemical properties different from those in the same layer under the polished surface. The depth of that layer is about ~ 70-100 nm. The implanted and the nearest layers are enriched with carbon that is conditioned by the HDII technology. Carbon is likely to exist as dispersion particles of TiC compound which strengthen the mentioned layers. Distribution of the chemical elements composition depends on sputtering time in $Ti_{49.5}Ni_{50.5}$ SMA. After a HDII treatment the sample surface is protected from crack formation [80].

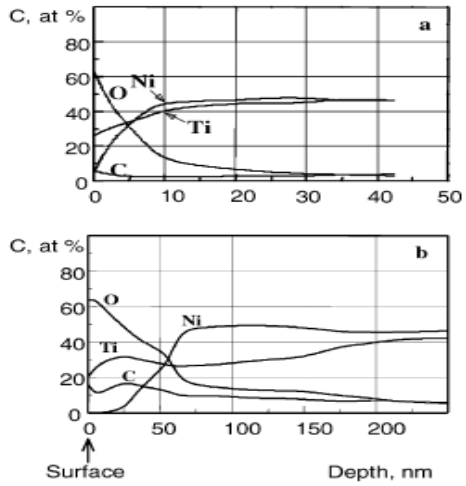

Figure (4). Distribution of the chemical elements composition depending on sputtering time in the $Ti_{49.5}Ni_{50.5}$ SMA with: (a) polished surface, and (b) implanted surface, Reference [78].

Deformed (4 % Tensile Strain) and undeformed martensite NiTi thin films, before irradiation with Au ions (Au^{+3}) (atomic weight 196.968) at 350 MeV, Fig. 5, indicate that the internally equilibrated residual stress remains after deformation [81].

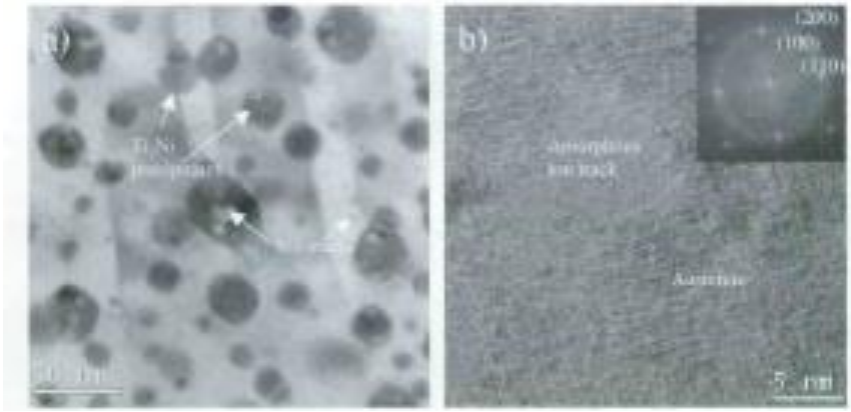

Figure (5). (a) Bright-field TEM image of 10^{12} Au ions cm^{-2} undeformed specimen that shows tracks (~ 10 nm Ø) in martensite and Ti_2Ni precipitates. (b) High-resolution TEM image of 10^{12} ions cm^{-2} undeformed specimen showing an austenite phase surrounding the tracks, Reference [79].

Ion tracks were observed in both martensite and the Ti_2Ni precipitates. The Ti-rich thin film microstructures contained a homogeneous distribution of Ti_2Ni phase within the grain Fig. 6a, and act as barriers and interrupt the growth of large variants, leading to a finer microstructure, causing the preferential development of (001) compound type twinning modes, which are less common in bulk materials, since the precipitates formed at the grain boundaries lead to poor mechanical properties. In thin films, these precipitates appear near grain boundaries. Closer examination (Fig. 6b) revealed that the tracks were surrounded by austenite with a lattice parameter of 0.305 nm, which is similar to the lattice constant calculated from the X-ray spectra determined from the inset fast Fourier transform (FFT) pattern [81].

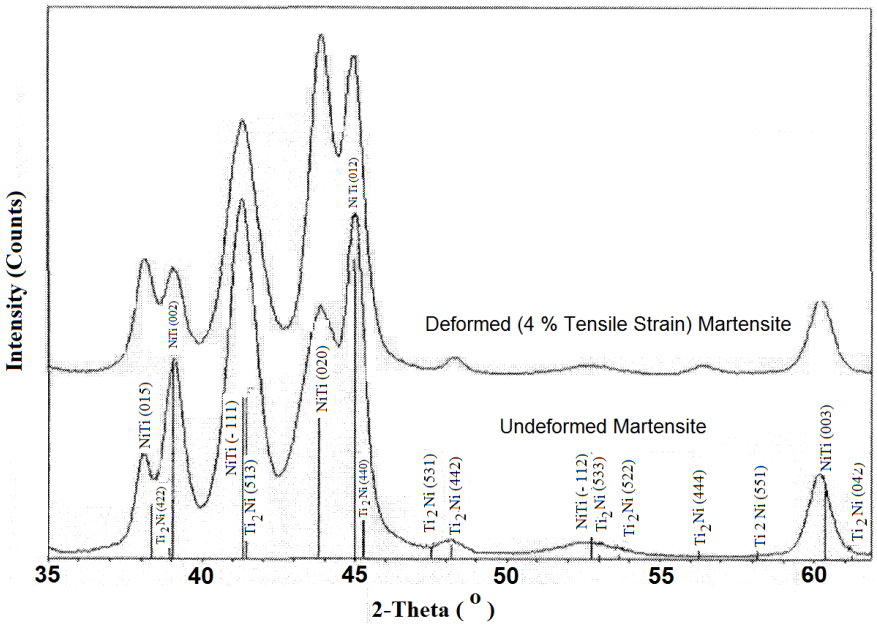

Figure (6). X-ray diffraction spectra showing the effects of deformation on the pre-irradiated microstructure by Au ions, Reference [79].

A grazing incidence X-ray diffraction spectra, Fig. 7, shows the result for three irradiation conditions (10^{12} Au ions cm^{-2} for deformed martensite, and both 10^{12} Au ions cm^{-2} and 10^{13} Au ions cm^{-2} for undeformed material), and confirms the presence of irradiation-induced *B*2-austenite phase. Splitting of the peak at ~ 42° indicates the formation of the R-phase. The slight broadening of the austenite diffraction peaks is observed for the 10^{13} ions cm^{-2} case, indicates an increase in the

amorphous material [81]. Table 3 shows the various phase volume fractions, calculated from integrated intensities using a pseudo-Voight peak profile fit and the Powder Cell and JADE 6.0 commercial XRD software packages, and both amorphization and stabilization of irradiation-induced austenite increase with both dose and pre-deformation.

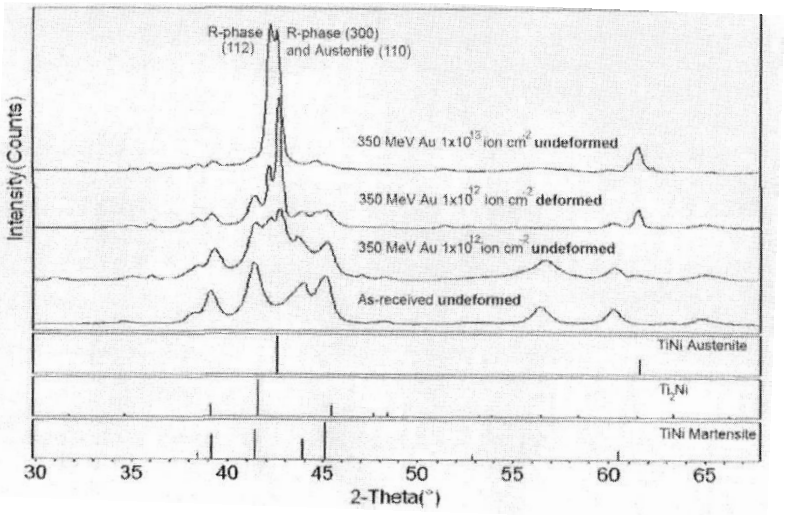

Figure (7). X-ray diffraction spectra for three irradiation conditions (10^{12} Au ions cm^{-2} for deformed martensite, and both 10^{12} Au ions cm^{-2} and 10^{13} Au ions cm^{-2} for undeformed material), showing effects 350 MeV Au ion irradiation, on the sputter deposited Ti-rich NiTi thin films, Reference [79].

Table (3). Phase volume phase fractions after Au ion irradiation, Reference [79].

Specimen	Martensite	Austenite	R Phase	Ti_2Ni	Amorphous
As-received	92.4	0	0	7.6	0
1×10^{12} undeformed	45.3	6.4	26.9	6.3	15.1
1×10^{13} undeformed	4.2	37.1	23.1	4.4	31.2
1×10^{12} deformed	27.7	10.2	27.7	5.1	29.3

DSC measurement analysis of transformation temperatures and enthalpie (H), where M_S, M_F, R_S, R_F, A_S, and A_F correspond to the martensite start, martensite finish, R-phase start, R-phase finish, austenite start and austenite finish, respectively. M_S, M_F and ΔH for the undeformed material decreased with increasing influence and depressed further in the deformed material as compared to the undeformed one for

the same irradiation dose, Table 4 [80]. Lagrange et al. [80] reported that the unirradiated martensite was stable up to ~ 60 ºC, indicating that the beam heating was not responsible for the observed transformation.

Table (4). Transformation temperatures of the TiNi SMA thin films before and after Au ion irradiation, Reference [79].

$H_{A\rightarrow M}$ Δ (J/g)	$H_{M\rightarrow A}$Δ (J/g)	A_F (ºC)	A_S (ºC)	R_F (ºC)	R_S (ºC)	M_F (ºC)	M_S (ºC)	Specimen
27.5	28.1	96.9	63.9	60.5	63.3	8.9	61.5	As-received
13.7	20.1	83.7	39.2	57.2	61.8	-10	37.8	1×10^{12} undeformed
13.1	16.9	64.4	41.5	47.7	53.3	-51.5	-16.6	1×10^{13} undeformed
16.6	19.7	75.2	52.5	57.9	60.4	-18.9	10	1×10^{13} deformed

4. Effect of Annealing and Aging on Ion-Implanted Nitinol Alloys

Electron, proton and neutron induced irradiation effects can be easily eliminated by annealing the specimens at 247 ºC or aging at room temperature for 76 days, [60], which confirms that the induced defects are temporary.

Amorphized TiNiCu specimens by Xe^+ irradiation were heated between 298 and 750 ºC for 10 min. [74]. The recovery process was observed by post-irradiation annealing experiment from room temperature to 750 ºC. The microstructure after the recrystallization is different from that of the unirradiated sample because they experienced different phase transformation: the former transformed from the amorphous phase and the latter came from the diffusionless martensitic transformation.

Post-irradiation annealing experiments indicate that no thermally activated crystallization occurred during Ni^+ irradiation at temperatures up to 250 ºC [77]. A full recovery of the original transformation characteristics was achieved after a short annealing of Ni^+ irradiated nitinol at 400 ºC for 30 min.

Shape memory effect can be obtained by solution treatment at high temperatures between 600 °C and 900 °C and subsequent aging at a temperature around 400 °C [82]. This aging process induces precipitation hardening of Ni-rich phases [83]. The transformation temperatures are elevated significantly as the matrix composition adjusts during aging [84].

5. Conclusion

From this review, we conclude that:

Ion implantation yields partial restoration phenomenon and recrystallization may happen in NiTi alloys. Internal interfaces and surfaces at internal pores are efficient sinks for the ion-induced defects. M_S, M_F and ΔH, for the undeformed material, decrease with increasing fluence of ion implantation and were depressed further for the deformed specimens at the same irradiation dose. Grazing incidence X-ray diffraction spectra confirm the presence of irradiation-induced *B*2-austenite. The observed slight broadening of the austenite diffraction peaks indicates an increase in the amorphous material. The total ion damage necessary to initiate the long-range disordering of bulk NC TiNi alloy is higher by a factor of at least one order of magnitude compared to polycrystalline TiNi, which is already partially amorphized at a dose of 0.4 dpa. No amorphization was detected at irradiation temperatures of 350 ^oC or higher, even after doses of 4 dpa. Irradiations to similar doses of Ni^{+2} ions at different temperatures showed that the amorphization kinetics slow down appreciably as the temperature is increased.

A special surface layer is formed, under the irradiated surface, with chemical properties different from those in the same layer under the polished surface. The depth of that layer is about ~ 70-100 nm. The implanted and the nearest layers are enriched with carbon which exist as dispersion particles of TiC compound which strengthen the mentioned layers and act as barriers and interrupt the growth of large variants, leading to a finer microstructure, causing the preferential development of (001) compound type twinning modes.

The long-range disordering of bulk NC TiNi alloy is at least one order of magnitude higher as compared to CG TiNi. A full recovery of the original transformation characteristics was achieved after a short annealing of Ni-ions irradiated nitinol at 400 ^oC for 30 min.

Aging processes induce precipitation hardening of Ni-rich phases, and the transformation temperatures are elevated significantly as the matrix composition adjusts during aging. Annealing at 277 ^oC initiates recrystallization and basically finishes at 750 ^oC. The crystallization temperature of amorphous alloys is significantly lowered by heavy ion and electron irradiation.

References

[1] **Ikuta, K**. "Modeling tools for the thermoelastic hysteretic behavior of SMA". *Ph.D. Thesis, Institute of Technology*, Tokyo (1987)

[2] **Ikuta, K.; Ichikawa, H.; Suzuki, K.; Yajima, D.** "Multi-degree of Freedom Hydraulic Pressure Driven Safety Active Catheter". *ICRA* (2006), 4161–4166.

[3] **Ikuta, K.; Hasegawa, T.; Daifu, S.** "Hyper redundant miniature manipulator "Hyper Finger" for remote minimally invasive surgery in deep area". *ICRA*, 1 (2003), 1098–1102.

[4] **Ikuta, K.; Yamamoto, K.; Sasaki, K.** "Development of remote microsurgery robot and newsurgical procedure for deep and narrow space". *ICRA* (2003), 1103–1108.

[5] **Ikuta, K.; Sasaki, K.; Yamamoto, K.; Shimada, T.** "Remote Microsurgery System for Deep and Narrow Space - Development of New Surgical Procedure and Microrobotic Tool". *MICCAI*. (2002), 163–172.

[6] **Poncet, P.** "Effect of constraining temperature on the postdeployment parameters ofself- expanding nitinol stents". *Proceedings of the International Conference on Shape Memory and Superelastic Technologies (SMST)* 441–455 (2000), 441–455.

[7] **Nakano, Y.; Fujie,M.; Hosada, Y.** "Hitachi's Robot Hand". *Robotics Age*, 6, (1984), 18–22.

[8] **Robertson, S. W.; Imbeni, V.; Notkina, E.; Wenk, H. -R.; Ritchie, R. O.** *Proceedings of SMAT conference, Menlo Park, CA*, (2003), 36.

[9] **Ikuta, K.; Tsukamoto,M.; Hirose, S.** Proceedings of 1988 IEEE Robotics and automation, Philadelphia, PA, (1987), 427–430.

[10]. **Bergamasco, M., Salsedo, F., Dario, P.** "A linear SMA motor as direct-drive robotic actuator". *IEEE International conference on Robotics and Automation, May, Scottdale, Arizona*, (1989), 618–623.

[11] **Hashimoto, M., Takeda, M., Sagawa, H., Chiba, I., Sato, K.** "Application of shape memory alloy torobo ticactuators". *J. Robotic Syst.*, 2, (1985), 3–25.

[12] **Hirosi, S., Ikuta, K., Umetani, Y.** "Development of SMA actuators perfomance assessment and introduction of a new composing approach". *Adv. Robotics*, 3, (1989), 3–16.

[13] **Hirosi, S., Ikuta, K., Umetani, Y.** Proceedings of the 5*th* CISMIFTOMM Symposium, Hermes Publishing, (1985), 339-349.

[14] **Hirosi, S., Ikuta, K., Sato, K.** "Developmental of a shape memory alloy actuator, improvement of output performance by the introduction of a-mechanism". *Adv. Robotics*, 3 (1989), 89–108.

[15] **Bergamasco, M., Salsedo, F., Dario, P. "**Shape memory alloy micromotors for direct- drive actuation of dexterous artificial hands". *Sens. Acutators***,** 17 (1989), 115–119.

[16] **Kuribayashi, K. "**Micro actuator using shape memory alloy for micro robot". Proceedings of IEEE Industrial Workshop and Advanced Motion Control, Ykohama, March (1990), 212–218.

[17] **Kuribayashi, K.** "A new actuator of a joint mechanism using TiNi alloy wire". *Int. Robotics Res.,* 4 (1986), 47–58.

[18] **Tanaka, Y., Yamada, A.** "A rotary actuator using shape memory alloy for robot-analysis of the response with load". *IEEE/RSJ International Workshop on Intelligent Robots and Systems". IROS 91, November 3–5,* Osaka, Japan (1991).

[19] **Dario, P., Buttazzo, G.** "An anthropomorphic robot finger for investigating artificial tactile perception". *Robotics Res.,* 6, 3 (1987), 25–48.

[20] **Ikuta, K**., **Tssukamoyo, M., Hirose S.** *Proceedings of IEEE International Conference on Robotics and Automation*, (1988), 427–430,

[21] **Golestaneh, A.** "Shape-memory phenomena". *Phys. Today,* 62 (1984), 70.

[22] **Saburi, T., Otsuka, K., Wayman, C.M. (eds.).** "TiNi shape memory alloys. Shape Memory Materials", Cambridge, (1998), 49–96.

[23] **Tang, W., Sundman, B., Sanström, R., Qiu, C.** "New modelling of the B2 phase and its associated martensitic transformation in the TiNi system". *Acta Mater.,* 47,12, (1999), 3457–3468.

[25] **Miller, D.A.; Lagouolas, D.C.** "Shape memory alloy servo aduator system with electric resistance feedback and application for active endoscope'. Influence of cold work and heat treatment on the shape memory effect and plastic strain development of NiTi". *Mater. Sci. Eng.,* A308, (2001), 161–175.

[26] **Eggeler, G., Allafi, J.K. Gollerthan, S.C., Somson, S., Schmahl, W., Sheptyakov, D.** "On the Effect of Aging on Martensitic Transformation in Ni-Rich NiTi Shape Memory alloys". *Smart Mater. Struct,* 14 (2005), S186–S191.

[27] **Pozzi, M., Airoldi, G.** "The electrical transport properties of shape memory alloys". *Mater. Sci. Eng.* A273–A275, (1999), 300–304.

[28] **Li, Y., Cui, L.S., Xu, H.B., Yang, D.Z.** "Constrained phase transformation of a TiNi shape-memory alloy". *Metall. Mater. Trans. A* 34A, (2003), 219–223.

[29] **Zheng, Y.m., Cui, L., Zhang, F. "**Effects of predeformation on the reverse martensitic transformation of NiTi shape memory alloy" *J. Mater. Sci. Technol,* 16, (2000), 611–614.

[30] **He, Z., Gall, K.R., Brinson, L.C.** *Matall. Mater. Trans.,* 37A (2006), 579.

[31] **Huang, X., Ackland G.J., Rabe, K.M.** "Crystal structures and shape memory behavior of NiTi". *Nat. Mater.,* 2, (2003), 307–311.

[32] **Chen, P.; Ting J.** "Characteristics of TiNi alloy thin films". *Thin Solid Films,* 398–399, (2001), 597–601.

[33] **Otsuka, K., Wayman, M.** Editors. "*Shape memory materials*", Cambridge University Press (1998). ISBN 0 521 44487 X (hc).

[34] **Yahia, L**. Editor. "*Shape Memory Implants*", New York, Spriger - Verlag (2000). ISBN 3 540 67229 – X

[35] **Kohl, M.** "*Shape memory micro actuators*", Springer, Berlin, Germany (2004). ISBN 3 540 20635 3.

[36] **Otsuka, K., Ren, X.** "Physical metallurgy of TiNi-based shape memory alloys". *Prog. Mater. Sci.,* 50, (2005) 511–678.

[37] **Yoneyama, T., Mayazaki, S.** (eds.) "*Shape memory alloys for biomedical applications*". Woodhead Publishing (2008).

[38] **Giurgiutiu, V., Zagrai, A.** "The use of smart materials technologies in radiation environment and nuclear industry". SPIE's 7th International Symposium on Smart Structures and Materials and 5th International Symposium on Nondstructive Evaluation and Health Monitoting of Aging Infrastructure, Newport Beach, CA., 5-9 March Paper (2000), 2985-103.

[39] **Luzzi, D.E., Mori, H., Fujita, H., Meshii, M.** "Driving force for amorphization of Cu_4Ti_3 by electron irradiation". *Scripta Metul.,* 19, (1985), 897–902.

[40] **Moine, P., Riviere, J.P., Ruault, M.O., Chaumont, J., Petton, A.** "In situ TEM study of martensitic NiTi amorphization by Ni ion implantation". *Sinclair Nucl. Inst. Meth.,* B718, (1985), 20–25.

[41] **Elliott, R.O., Koss, D.A.** "Amorphization of Pu_5Ga_3 by neutron irradiation". *Nucl. Mater.,* 97, (1981), 339–441.

[42] **Bloch, J.** "Effet del' irradiation par les neutrons sur les alliages uranium-fer a faible teneur en fer". *Nucl. Mater.* 6(2), (1962), 203.

[43] **Tolley, A.** "The effect of electron irradiation on the $\beta \Leftrightarrow$18R martensitic transformation in Cu-Zn-Al alloys". *Radiat. Eff. Defects Solids,* 128, (1994, 229-245.

[44] **Brimhall, J.L.** "Effect of irradiation particle mass on crystallization of amorphous alloys". *Mater. Sci.,* 19, (1984), 1818-1826.

[45] **Maziasz, P.J., Pedraza, D.F., Simmons, J.P., Packon, N.H.,** "Temperature dependence of the amorphization of NiTi irradiated with Ni ions". *Mater. Research,* 5, (1990), 932-941.

[46] **Kinoshita, C. "**Electron irradiation-induced transformations in alloys and ceramics". *Electron Microscopy***,** 34, (1984), 299-310.

[47] **Saito, K.** "Transformation characteristics in thin foils of a nickel-titanium alloy". *Radiation Effects and Defects in Solids,* 79, (1983), 29-41.

[48] ***Mori, H., Fujita, H. "****Temperature dependence of electron-irradiation induced amorphization of NiTi alloys".* Jpn. J. Appl. Phys., *21, (1982*), *L494. DOI :10.1143/JJAP.21.L494*

[49] ***Matsukawa, Y., Ohnuki, S.*** *"Electron irradiation effect on the phase transformation in Ti- Ni shape memory alloy".* Nucl. Mater., *239, (1996), 261-266.*

[50] **Zu, X.T., Wang, L. M., Huo, Y., Lin, L.B., Wang, Z.G., Lu, T.C., Liu, L.J., Feng, X.D**. "Effect of electron irradiation on the transformation characteristics of narrow hysteresis TiNiCu shape memory alloys". *Appl. Phys. Lett.***,** 80, (2002), 31-33.

1) [51] **Zu, X.T.,Wan, F.R., Zhu, S., Wang, L.M.** "In situ TEM study of irradiation-induced transformation in TiNi shape memory alloys". *Mat. Res. Soc. Symp. Proc.*, 792, (2004), R1.10.1 DOI: http://dx.doi.org./101557/PROC-792-R1.10

2) [52] **Zu, X.T., Lin, L.B., Wang, Z.G., Zhu, S.; You, L.P., Wang, L.M., Huo, Y.** "Influence of electron irradiation on the martensitic transformation of a binary TiNi shape memory alloy". *J. Alloys and Compounds*, 351, (2003), 87-90.

[53] **Liu, Y., McCormick, P.G. "**Thermodynamic analysis of the martensitic transformation in NiTi—I. Effect of heat treatment on transformation behavior". *Scripta Metall. Mater.*, 42, (1994), 2401-2406.

[54] **Zu, X.T., Wan, F.R., Zhu, S., Wang, L.M.** "Irradiation-induced martensitic transformation of TiNi shape memory alloys". *Physica B* 351, (2004), 59-62.

[55] **Wang, Z.G., Zu, X.T., Fu, Y.Q., Zhu, S.,** Wang, L.M. "Electron irradiation effect on the reverse phase transformation temperatures in TiNi shape memory alloy thin films". *Nuclear Inst. Meth. Phys. Res.*, B227, (2005), 337-342.

[56] **Dughaish, Z.H.** "Effect of proton Irradiation on some physical properties of nitinol (NiTi) shape memory alloy. a review". *Arab J. Sci. Eng.*,39, (2014), 511–524 DOI: 10.1007/s13369-013-0878-5.

[57] **Al-Aql, A.A., Dughaish, Z.H., Baig, M.R. "**Study of the martensitic transformation in shape-memory nitinol proton-irradiated alloy by electrical resistivity measurements". *Mater. Lett.*, 17, (1993), 103-108.

[58] **Al-Aql, A.A., Dughaish, Z.H., Baig, M.R., Hassib, A. M. "**Effect of aging and annealing on the electrical resistivity of proton irradiated nitinol". *Physica B*, 210, (1995), 87-90.

[59] **Al-Aql, A.A., Dughaish, Z.H.** "Effect of energy variation of proton beam on sharpening nitinol electrical resistivity increase at the martensitic transformation". *Physica B,* 229, (1996), 91-95.

[60] **Dughaish, Z.H. "**Effect of variation of proton beam energy on the martensitic transformation temperature of shape memory nitinol alloy". *Mater. Lett.* 32, (1997), 29-32.

[61] **Wang, Z.G., Zu, X.T., Zhu, S., Huo, Y., Lin, L.B., Feng, X.D.,Wang, L.M**. "Effect of 18 MeV proton irradiation on the R-phase transformation in TiNi shape memory alloys". *Nuclear Instruments and Methods in Physical Research,* B211, (2003), 239-243.

[62] **Kimura, A., Tsuruga, H., Morimura, T., Miyazaki, S., Misawa, T.** "Effect of post-irradiation annealing on the transformation behavior of Ti-Ni alloys". *Mater. Trans. JIM* **,**34, (1993), 1076-1082.

[63] **Nakata, Y., Tadaki, T., Shimizu, K.** *MRS International on Advances in Materials, 9, Material Research Society,* (1989), 231-236.

[64] **Matsukawa, Y., Suda, T., Ohnuki, S., Namba, C.,** "Microstructure and mechanical properties of neutron irradiated TiNi shape memory alloy". *Nuclear Materials,* 271-272, (1999), 106-110.

[65] **Al-Aql, A. A. "**Effect of neutron irradiation on transformation temperatures of nearly equi-atomic nitinol alloys". *J. King Saud Univ. Science,* 12 (2), (2000), 123-128.

[66] **Ma Benjamin, Y. M.** "*Nuclear reactor materials and application"*, Van Nostrand Reinhold Co., New York, (1983), 61.

[67] **Cohen, M., Olson, G.B. "**A mechanism for the strain-induced nucleation of martensitic transformations". *Less-Common Met*., 28, (1972), 107-118.

[68] **Cheng, J., Ardell A.J. "**Proton-irradiation-induced crystalline to morphous transition in a NiTi alloy". *Nuclear Instruments and Methods in Physics Research Section* B44, (1990), 336-343.

[69] **Goldberg, F., Knystautas, E.J.** "The effects of ion irradiation on NiTi shape memory alloy thin films". *Thin Solid Films* 342, (1999), 67-73.

[70] **Sergueeva, A.V., Song, C., Valiev, R.Z., Mukherjee, A.K. "**Structure and properties of amorphous and nanocrystalline NiTi prepared by severe plastic deformation and annealing". *Mater.Sci. Eng.*. A 339, (2003), 159-165.

[71] **Nita, N., Schaeublin, R., Vectoria, M., Valiev. R.Z.** "Effects of irradiation on the microstructure and mechanical properties of nanostructured materials". *Philos. Mag.,* 85, (2005), 723-735.

[72] **Goldberg, F.** "*Ph.D. Thesis, Université Laval*", (1998), 154.

[73] **Kilmametov, A.R., Gunderov, D.V., Valiev, R.Z., Balogh, A.G., Hahn, H.** "Enhanced ion irradiation resistance of bulk nanocrystalline TiNi alloy". *Scripta Materialia* 59, (2008), 1027-1030.

[74] **Rose, M., Balogh, A.G., Hahn, H.** "Instability of irradiation induced defects in nanostructured materials". *Nucl. Inst. Methods* B127 & 128, (1997), 119-122.

[75] **Zu, X.T., Zhu, S., Xiang, X., You, L.P., Huo, Y., Wang, L.M.** "In situ TEM observation of heavy-ion-irradiation-induced amorphization in a TiNiCu shape memory alloy". *Mater. Sci. and Eng.*, A363, (2003), 352-355.

[76] **Pelletier, H., Muller, D.,Mille, P., Grob. J.J. "**Structural and mechanical characterisation of boron and nitrogen implanted NiTi shape memory alloy". *Surface and Coating Technology* 158-159, (2002), 309-317.

[77] **Wentzel, A., Hammerl, C., Königer, A., Rauschenbach B.** "Formation of titanium carbide by high-fluence carbon ion implantation". *Nucl; Instr. Meth.* B129 (1997), 369-376.

[78] **LaGrange, T., Gotthardt, R.,** "Post-annealing of ion irradiated TiNi SMA thin films". *Mater. Sci. Eng*., A378, (2004), 448-452.

[79] **LaGrange, T.B., Grummon, D.S., Gotthardt, R. "**The influence of irradiation parameters on the behavior of martensitic titanium nickel thin films". *Optoelectron. Adv. Mater*., 5, (2003), 313-318.

[80] **Meisner, L.L., Sivokha, V.P., Lotkov, A.I., Derevyagina, L.A.** "Surface morphology and plastic deformation of the ion-implanted TiNi alloy". *Physica B*, 307, (2001) , 251-257.

[81] **LaGrange, T., Schaublin, R., Grummon, D.S., Abromeit, C., Gotthardt, R. "**Irradiation-induced phase transformation in undeformed and deformed NiTi shape memory thin films by high-energy ion beams". *Phil. Mag.* 85, (2005), 577-587.

[82] **Ming, H.Wu. "**Fabrication of nitinol materials and components". *Proceedings, International Conference on Shape Memory and Superelasticity Technologies*, Kunming, China, (2001), 285-292.

[83] **Miyazaki, S, Kimura, S., Takei, F., Miura, T., Otsuka, K., Suzuki, Y**., "Shape memory effect and pseudoelasticity in a TiNi single crystal". *Scripta Metall.* 17, (1983), 1057-1062.

[84] **Lee, J.H., Lee, H.W., Ahn, J.G., Chung H.K., Song, K.** *Proceedings, International Conference on Shape Memory and Superelasticity Technologies*, Antwerp, Belgium (1999) 33.

تأثير الغرس الايونى على بعض الصفات الفيزيائية للنيتينول (Ni-Ti) سبيكة ذات الشكل المختزن

زباد حسين دغيش المصرى

قسم الفيزياء –كلية العلوم – جامعة القصيم ص ب ٦٦٤٤ بريدة ٥١٤٥٢ القصيم

البريد الإلكتروني Zhdalmas45@gmail.com - msary@qu.edu.sa

ملخص البحث. إن السبائك ذات الشكل المختزن (المرتجع) نوع خاص من السبائك المعدنية التي بإمكانها، بعد تشوهها تشوهاً كبيراً، أن تستعيد شكلها الأصلي بعملية التسخين. إن سلوكها غير الخطي واعتمادها على الحرارة، قد جذب عدداً كبيراً من الباحثين والمهندسين والمصممين لاختيار أنسب المواد وأفضلها للتطبيقات المناسبة في حقول صناعية مختلفة. إن سبيكة النيتينول هي أكثر هذه السبائك استعمالاً. وهي سبيكة غير سامة وخواصها مناسبة لاستعمالها في تجبير الكسور العظمية، ونظراً لخواصها المتميزة فإنها تدخل في العمليات التي تستخدم أجهزة طبية نادرة. إذ تستعمل أنابيب مصنعة من سبيكة النيتينول كثيراً في عمليات القسطرة والشبكات والإبر فائقة المرونة وفي أجهزة توصيل وإعادة ربط الأمعاء بعد إزالة الجزء المصاب. كما يستعمل النيتينول في كثير من الأجهزة الطبية، والقواطع الكهربائية والصناعات الروبوتية، والمفاعلات النووية، والبيئة الإشعاعية والصناعة النووية وغيرها من التطبيقات. تتعرض سبيكة النيتينول أثناء استخدامها في المفاعلات النووية لأنواع مختلفة من الإشعاعات والتي قد تؤثر على خواصها وتركيبها. ونقدم هنا مراجعة لمجموعة من تقارير عن بحوث سابقة عديدة حول تأثير الغرس الأيوني في النيتينول بكتل وطاقات مختلفة من الأيونات He^{+}, B^{+}, C^{+}, N^{+}, Ar^{+}, Xe^{+}, Ti^{+2}, Ni^{+2}, Cu^{+2}, Au^{+3} على خواصها المختلفة. آملاً ان تتم بها الفائدة وتقدم مساعدة ومنفعة للباحثين والمهندسين العاملين في هذا الحقل.

الكلمات المفتاحية : السبائك ذات الشكل المختزن– نيتينول – اثار التشعيع –الغرس الايونى – التغير المارتنزيتى